

Rydberg stabilization of atoms in strong fields: the “magic mountain” in the chaotic sea

Francesco Benvenuto¹, Giulio Casati^{1,*}, D.L. Shepelyansky^{2,**}

¹ Dipartimento di Fisica dell'Università, Via Castelnovo 7, I-22100 Como, Italy

² Laboratoire de Physique Quantique, Université Paul Sabatier, F-31062 Toulouse, France

Received: 6 October 1993 / Revised version: 29 December 1993

Abstract. We discuss the classical problem of an hydrogen atom interacting with a monochromatic field. We illustrate in particular, analytically and numerically, the stabilization mechanism and give theoretical expressions for the stabilization borders.

PACS: 31.50.+w; 32.80.Rm; 42.50.Hz

The effect of a monochromatic perturbation on the Kepler motion is certainly a basic problem in theoretical physics. In particular it is relevant for the understanding of the excitation and ionization process of hydrogen atoms under microwave or laser fields. Even though the latter problem is strictly a quantum one a classical description turns out to be crucial for the understanding of the physical process. Due to its importance and formal simplicity this problem is well studied and the properties of the motion are already known to large extent.

The classical motion is described, in cylindrical coordinates, by the following simple Hamiltonian:

$$H = \frac{1}{2}(p_\rho^2 + p_z^2) + \frac{m^2}{2\rho^2} - \frac{1}{\sqrt{\rho^2 + z^2}} + \varepsilon z \cos \omega t; \quad (1)$$

where z is the direction of the linearly-polarized external field, m is the projection of the angular momentum on the field direction, ε and ω are the intensity and frequency of the field. Here and in the following we will use atomic units.

Theoretical and numerical results show that for $\omega_0 = \omega n_0^3 > 1$ where n_0 is the initially excited state, and

* Also at: Istituto Nazionale di Fisica Nucleare, Sezione di Milano, Milano, Italy

** Also at: Budker Institute of Nuclear Physics, 630090 Novosibirsk, Russia

for field strength $\varepsilon_0 = \varepsilon n_0^4 > \varepsilon_c \approx (50 \omega_0^{1/3})^{-1}$, the electron motion enters a chaotic regime which leads to a diffusive process in action space and then to ionization [1]. For $\omega_0 < 1$ the critical field for ionization increases and for $\omega_0 \rightarrow 0$ it approaches the static field value $\varepsilon_0 \approx 0.13$.

Notice that for $\omega_0 > 1$ and when the electron is far from the nucleus, the external field mainly leads only to oscillations of the electron around its average Kepler orbit. Near the perihelion, instead, the electron motion is strongly perturbed due to the Coulomb singularity: therefore the influence of the external perturbation can be described as a sequence of kicks. For this reason it was possible to describe the classical (and the quantum) motion by a map: the Kepler map [1]. Such Kepler map, which was originally introduced to describe the one-dimensional model, provides a very useful insight on the nature of classical motion; it gives the change in energy after one orbital period, and has the simple form:

$$\begin{aligned} \bar{N} &= N + k \sin \Phi, \\ \bar{\Phi} &= \Phi + 2\pi\omega (-2\omega\bar{N})^{-3/2}; \end{aligned} \quad (2)$$

where $N = E/\omega = -(2n^2\omega)^{-1}$, and ϕ is the field phase at perihelion. The bar denotes the new values of variables after one orbital period, and the parameter $k \approx 2.6 \varepsilon \omega^{-5/3}$. The map (2) provides a good approximation of the motion for $\omega_0 \geq 1$, while in the opposite situation, $\omega_0 \ll 1$ ionization behaves almost in the same way as in the static field case.

Even though map (2) was derived for the 1D case, it was shown to give a quite good qualitative description even for the full 3D case (with parameter k slowly depending on l) provided the orbital momentum $l < (3/\omega)^{1/3}$ [1].

The Kepler map approach allows to easily understand the process of transition to the continuum. Indeed, when one of the kicks brings the electron in the positive energy region, ionization takes place: in the physical space the electron will proceed to infinity and never come back. Quite obviously, above the chaos border, the diffusive ionization rate depends upon the value of parameters.

More precisely, according to simple estimates [1] the ionization time τ_I , measured as the number of elapsed field periods, is $\tau_I \sim \omega_0^{7/3} \varepsilon_0^{-2}$.

However, the Kepler map description is only valid provided the field is not too strong. As a matter of fact, map (2) was derived under the assumption that the energy change caused by one kick $\Delta E \sim k\omega$ is much larger than the energy of free oscillations $\varepsilon^2/(2\omega^2)$, namely:

$$\varepsilon \ll \varepsilon_{ATI} \approx 5\omega^{4/3}. \quad (3)$$

The qualitative behavior for larger fields strictly depends on dimensionality. For the 1D case with strong fields $\varepsilon \gg \varepsilon_{ATI}$, the unavoidable collisions with the nucleus will lead to ionization. A similar argument holds for the 2D case ($m=0$); here, for $l > (3/\omega)^{1/3}$ the k value in (2) becomes exponentially small and therefore atoms remain stable up to very high field strength until the amplitude of free oscillations ε/ω^2 becomes larger than the unperturbed distance between the electron and the nucleus at perihelion $l^2/2$. Therefore, as it was shown in [2], for $m=0$ a critical field value always exists (which may be very large when the angular momentum l is large) below which the atom is stable, and above which ionization takes place.

The most interesting case occurs for $m \neq 0$, and for sufficiently strong fields, so that the Kepler map description is not valid. Here the centrifugal potential makes it possible to avoid collisions between the electron and the nucleus, thus preventing ionization. Indeed, by increasing the external field, the amplitude of the free oscillations is also increased, thus leading to a decrease of the attracting Coulomb force, while the centrifugal force remains the same. Therefore the distance between the electron and the nucleus will increase with the increase of the field. This fact suggests the possibility that atoms will become stable by increasing field intensity.

Actually this phenomenon, called “stabilization”, was put forward for the quantum case [3–5]. Theoretical arguments were given to predict that a quantum atom should become stable when the energy of field photon is much larger than the coupling energy and when the size of electron oscillations in the field ε/ω^2 is much larger than the size of the atom [8]. These conditions are of purely quantum nature and according to them there is no stabilization in the classical atom. Indeed in the quasi-classical limit the energy of one photon $\hbar\omega$ goes to zero and becomes much smaller than the energy required for ionization, which is independent on \hbar .

On the base of our arguments we expect stabilization to take place in the classical atom. As a matter of fact we were able to derive an analytical expression for the stabilization border [9] which shows that stabilization is present in the purely classical context even when the size ε/ω^2 of electron oscillations in the field is much less than the size of the atom. Due to the correspondence principle, the existence of classical stabilization implies in particular that stabilization in quantum case will take place even when the photon energy $\hbar\omega$ is less than the coupling energy of the atom.

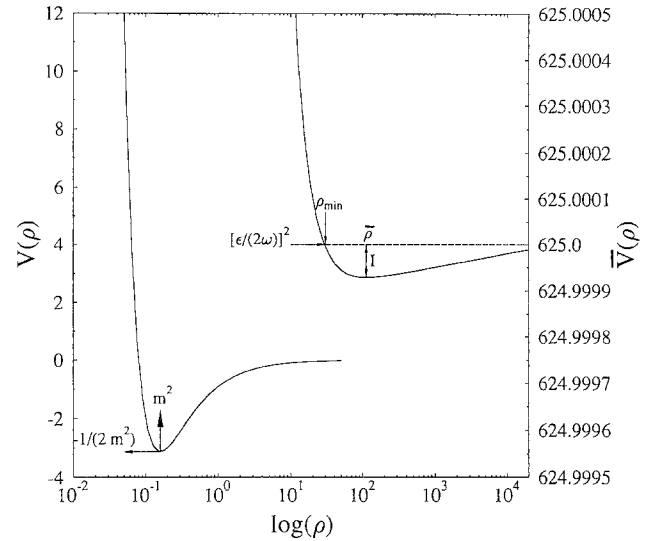


Fig. 1. The potential $V(\rho)$ for small ρ taken at $z=0$ (left part), and the “effective” average potential $\bar{V}(\rho)$ for large ρ (right part). The left and right vertical scales are different. Here $\bar{\rho} = \sqrt{\frac{\pi\varepsilon}{2} \frac{m}{\omega}}$, $\rho_{\min} = \sqrt{\frac{\pi\varepsilon}{L} \frac{m}{2\omega}}$ and $I = \frac{2\omega^2}{\pi\varepsilon} L$. The curves are drawn for $\omega = 0.001$, $m = 0.4$, $\varepsilon = 0.05$

To better understand the features of the classical motion it is convenient to focus our attention on the dynamics in the ρ -direction. From Hamiltonian (1) one can see that when both ε and ρ are sufficiently large, the z -motion is dominated by the driving term giving approximately $z \approx \varepsilon/\omega^2 \cos(\omega t)$. One can then average over the z -motion and obtain an Hamiltonian which describes the average motion in ρ ; the effective averaged potential $\bar{V}(\rho)$ has a minimum in $\bar{\rho} = \sqrt{\pi\varepsilon/2} (m/\omega)$ and near $z=0$ can be approximately written as (Fig. 1):

$$\bar{V}(\rho) = \frac{m^2}{2\rho^2} + \frac{2\omega^2}{\pi\varepsilon} \log\left(\frac{\rho\omega^2}{\varepsilon}\right) + \frac{1}{4} \left(\frac{\varepsilon}{\omega}\right)^2. \quad (4)$$

Notice that the logarithmic term gives the local potential of a charged thread which arises due to electron oscillations. Expression (4) is valid as long as $\rho < \varepsilon/\omega^2$; for larger ρ values the average potential approaches the asymptotic constant value $1/4(\varepsilon/\omega^2)$ (see the right part of Fig. 1 where the averaged potential is shown).

The average potential (4) gives a good description of the electron motion if the frequency $\Omega \approx \omega^2/(\varepsilon m)$ of oscillations in ρ is much smaller than the frequency ω of field oscillations. This condition, namely $S = \omega/\Omega \gg 1$, is fulfilled if

$$\varepsilon > \varepsilon_{\text{stab}} = \beta \frac{\omega}{m} \quad (5)$$

where β is a numerical constant. We call S the “stabilization parameter”. In the quantum case the substitution of m by $m+1$ is needed in order to take in account that quantum effects smooth the singularity, and that semi-classical quantization gives non zero m value (see also the discussion in [10, 11]).

Therefore, under condition (5), the atom is stable since the averaged Hamiltonian

$$\bar{H} = \frac{p_\rho^2}{2} + \bar{V}(\rho) \tag{6}$$

is a constant of the motion with adiabatic accuracy [$\approx \exp(-\text{const} \cdot S)$]. For field values smaller than (5) down to the usual chaos border, ionization takes place. Numerical computations [9] confirmed the estimate (5) with $\beta \approx 12$.

The stabilization border (5) is much higher than the chaos and static ionization borders. Therefore in order to obtain atoms in the stabilized region attention must be paid to the field switching process. Namely, the time of switching t_s must be less than the orbital period of the electron $2\pi n^3$ and moreover $\int_0^{t_s} \varepsilon(t) dt \approx 0$, so that the field does not transfer momentum to the electron during the switching time. With such type of switching and for initial unperturbed state n_0 , the size $2n_0^2$ of the initial atom in sufficiently strong fields becomes smaller than $\rho_{\min} = \frac{m}{2\omega} \left(\frac{\pi\varepsilon}{L}\right)^{1/2}$ and therefore the electron cannot be cap-

tured in the minimum of the averaged potential (see Fig. 1), hence ionization takes place after one orbital period. This gives the destabilization border:

$$\varepsilon_{\text{dest}} \approx \frac{16L\omega_0^2}{\pi m^2 n_0^2} \tag{7}$$

where

$$L = \ln \left[\left(\frac{2\varepsilon}{e\pi} \right)^{1/2} \frac{1}{\omega m} \right].$$

Notice that the stabilization border (5) is relevant only if $\omega m^3 < 3$. Indeed in the opposite case the electron passes sufficiently far from the nucleus and the change of energy during these passages are exponentially small and atoms remain stable up to the value given by (7). This fact is in agreement with the numerical simulations [10].

In Fig. 2 we present a general picture of the stability diagram in the $(\varepsilon_0, \frac{\omega_0}{m_0})$ plane. The most impressive result of our analysis is the “magic mountain” of stability in the upper-rightmost part of the figure which emerges from the chaotic sea and, coming from infinity, approaches, but does not touch, the familiar territory of K.A.M. stability. The latter is delimited by the full curve in the lower part of Fig. 2. Quite obviously the details of the classical motion depend separately on all parameters m, ε, ω , as well as on the initial conditions, however Fig. 2 gives the correct main qualitative behavior.

The three dashed lines on Fig. 2 are drawn at three different values of ε . One can move along these lines by changing n_0 only (ε, ω, m fixed), and the corresponding different types of motion are illustrated on Fig. 3, in which we draw the related surfaces of section in the (ρ, p_ρ) plane. To this end we numerically integrate system (1) and plot the intersections of the orbit with the (ρ, p_ρ) plane at each microwave period. Since we are dealing with a two degrees of freedom system, periodically perturbed, we should not expect to obtain smooth curves even in the quasi-integrable stable region; still useful informations can be obtained on the qualitative properties of the motion. For reason of graphical presentation we use two different vertical scales and the dashed vertical line in Figs. 3a–3b is drawn only to separate these two scales. In Fig. 3c, only the points in the upper curve, corresponding to $n_0 = 1$, refer to the left scale, while all the other curves refer to the right scale.

From the inspection of Fig. 2 one can easily predict the qualitative behavior of the solutions of system (1). Indeed for $\varepsilon = 0.0025$ (line *a*) there is a chaos border at $n_0 \geq 2$ below which the orbits are stable and above which orbits ionize. For $\varepsilon = 0.05$ (line *b*) the chaos border is around $n_0 \geq 1$; in the range $1 < n_0 \leq 6$ orbits ionize, while for $n_0 > 7$ orbits are stable again. For $\varepsilon = 1$ (line *c*) the K.A.M. stable region disappears since here $m = 0.4$ is fixed and n_0 must be larger than m ; therefore all orbits with $n_0 \leq \bar{n}$ ionize, while orbits with $n_0 \geq \bar{n}$ are stable, where $\bar{n} \approx 12$. The latter dependence of ionization on initial conditions at fixed ε, ω, m is probably the most surprising effect of stabilization. These predictions are confirmed

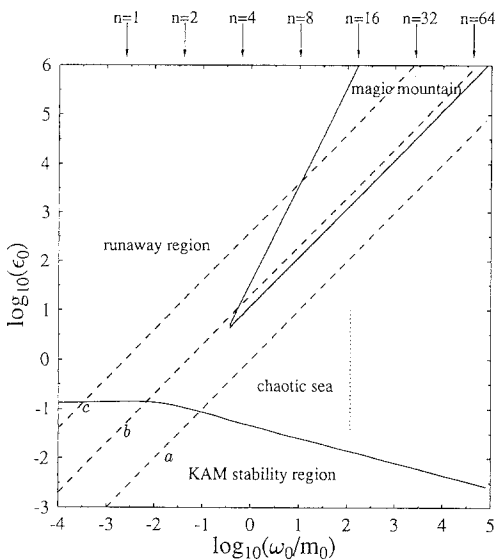


Fig. 2. The stability borders for Hamiltonian (1) at fixed $\omega = 0.001$ and $m = 0.4$. The lower curve is the usual chaos border $\varepsilon_0 \approx \frac{1}{50\omega_0^{1/3}} = \frac{1}{50(\omega m^3)^{1/12}} \left(\frac{m_0}{\omega_0}\right)^{1/4}$. For small ω_0 this border approaches the usual static border $\varepsilon_0 \approx 0.13$. The “magic mountain” of stability is delimited from below by the stabilization border $\varepsilon_0 \approx 12 \frac{\omega_0}{m_0}$ and from above by the destabilization border $\varepsilon_0 \approx \frac{16L}{\pi} \left(\frac{\omega_0}{m_0}\right)^2$ with $L = \ln \left(\sqrt{\frac{2}{e\pi}} \sqrt{\frac{\varepsilon_0}{\omega_0 m_0}} \right)$. The dashed lines $\varepsilon_0 = \left(\frac{\varepsilon}{m}\right) \left(\frac{\omega_0}{m_0}\right)$ are drawn at constant ε : (a) $\varepsilon = 0.0025$; (b) $\varepsilon = 0.05$; (c) $\varepsilon = 1$. The border (3) below which the Kepler map description is valid is given, in the present case, with fixed m and ω , by the line $\varepsilon_0 = 0.2 \left(\frac{\omega_0}{m_0}\right)$ (not drawn in the figure). The present picture is drawn at fixed ω and m . If instead we keep n_0 fixed, then the system will always be stable in the region to the right of the dotted vertical line given by $\omega_0 m_0^3 = 3$

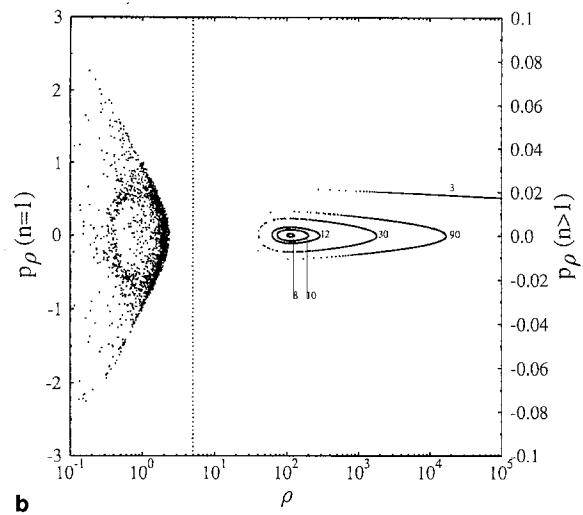
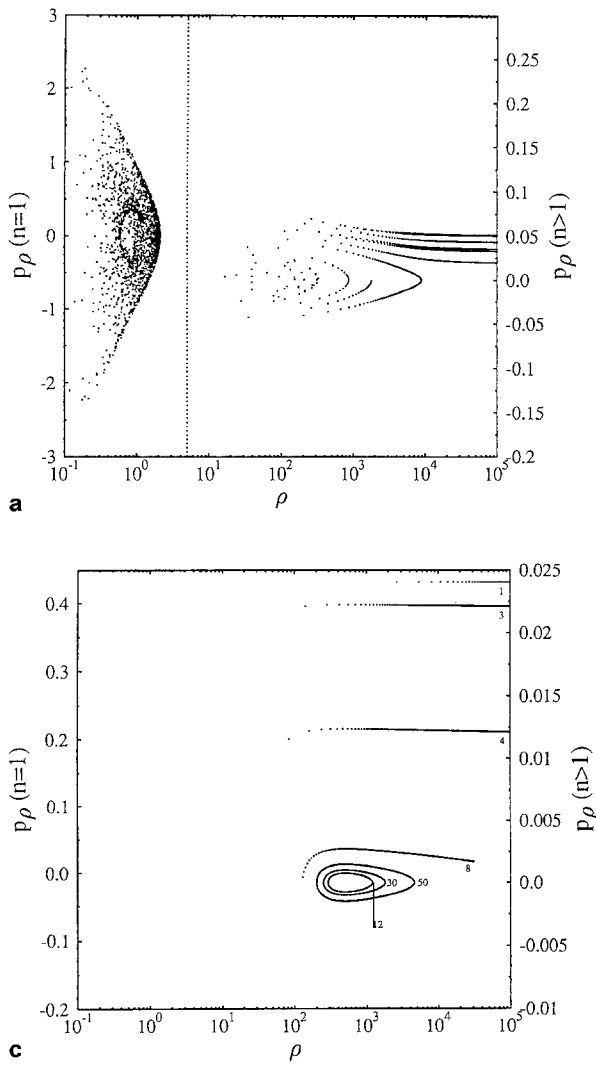


Fig. 3. Surfaces of section plots obtained by solving system (1) for the three different cases of Fig. 2 with $\omega = 0.001$, $l = m = 0.4$; **a** $\varepsilon = 0.0025$, **b** $\varepsilon = 0.05$, **c** $\varepsilon = 1$. The curves are obtained by plotting the values (ρ, p_ρ) after each period of the external field. The dotted vertical line in Fig. 3a, b separate the two different scales on the vertical axis. The different set of points (curves) refer to different values of initial classical action n . In Fig. 3a only the orbit with $n = 1$ is stable and all the others with $n = 3, 4, 8, 10, 12, 30$ ionize. In Fig. 3b the orbit with $n = 3$ ionizes, all the others are stable. In Fig. 3c the orbits with $n = 1, 3, 4, 8$ ionize, while those with $n = 12, 30, 50$ are stable; here only the points in the upper curve, corresponding to $n = 1$ refer to the scale on the left axis, while all the other curves refer to the right scale

by Figs. 3a–3c where the two minima of the potential in Fig. 1 are clearly seen. The points to the left in Figs. 3a–3b belonging to $n_0 = 1$, are centered around $\rho \approx m^2 = 0.16$ and the excursion in p_0 is $\approx 1/m = 2.5$. The points to the right, belonging to $n_0 \geq 3$ are centered around $\bar{\rho} \approx \sqrt{\pi \varepsilon / 2} (m/\omega) \approx 500 \sqrt{\varepsilon}$ which is the position of the minimum in the potential (4).

An interesting remark is that the low frequency case is qualitatively different from the static field case limit. Indeed for the static case the electron can remain stable only near the nucleus. Instead, in the case of a monochromatic field with small frequency ω , the stabilization border (5) is very low and new stable minimum appears at ρ_{\min} far from the nucleus.

The general picture of classical motion we give in Fig. 2 leads to different conclusions than those existing in the current literature. One point to be stressed is that the main effect on the electron, produced by the collision with the nucleus, is in the perpendicular ρ -direction while in the z -direction the velocity changes only slightly. This is a typical situation for the collision of a fast heavy particle with a light electron: the momentum of the electron in z -direction remains practically unchanged. This consideration allows to construct an approximate 1D model [11]. Indeed, in the Kramers-Henneberger frame [18] Hamiltonian (1) writes

$$H = \frac{p_z^2}{2} + \frac{p_\rho^2}{2} + \frac{m^2}{2\rho^2} - \frac{1}{\sqrt{\rho^2 + \left(z - \frac{\varepsilon}{\omega^2} \sin \omega t\right)^2}}. \quad (8)$$

Neglecting the changes in z we may write the following, approximate, 1D Hamiltonian

$$H = \frac{p_\rho^2}{2} + \frac{m^2}{2\rho^2} - \frac{1}{\sqrt{\rho^2 + \frac{\varepsilon^2}{\omega^4} (\sin \gamma + \sin \omega t)^2}} \quad (9)$$

where γ is a constant which determines the point of collision in $z = -\varepsilon \sin \gamma / \omega^2$. This Hamiltonian is quite different from the usual 1D screened Coulomb model [4] which is frequently used to approximate the 3D dynamics and leads to results which are in quite good agreement with the full 3D dynamics. Indeed Fig. 4 shows an example of a surface of section plot obtained from Hamiltonian (9) with the same parameters as in Fig. 3b. The curves in Fig. 4 completely overlap with the corresponding curves in the right part of Fig. 3b thus indicating that the approximate Hamiltonian (9) gives quite an accurate description of the real motion. Needless to say, while Hamiltonian (9) is accurate for the description of the stabilization phenomenon, it cannot certainly de-

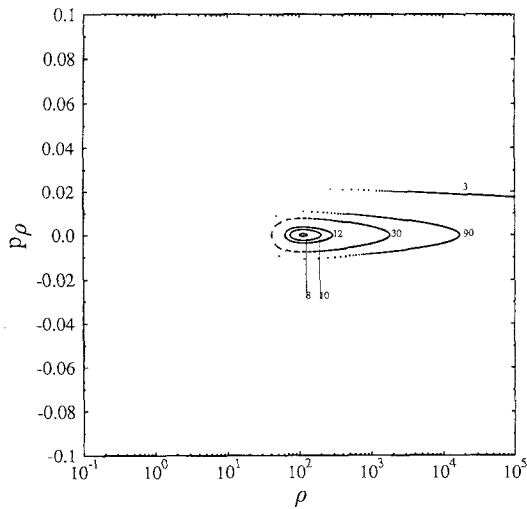


Fig. 4. Surface of section plot for the case of Fig. 3b, obtained by solving the 1D approximate Hamiltonian (9) with $\sin \gamma = 0.6$. Notice the good agreement with the curves of Fig. 3b obtained from the numerical solution of the exact Hamiltonian (1)

scribe the motion in the K.A.M. region, in the left part of Fig. 3b where the electron closely follows the nucleus oscillations.

In order to provide the reader with a more complete picture of the stabilization phenomenon, we would like to make a few comments on other existing theories. The first step in this direction is to define, as clearly as possible, the meaning of the term “stabilization”. As it is clear from the above discussion, under the term stabilization we mean that atoms are stable in sufficiently strong fields while they are ionized for smaller fields. Moreover, by stable we mean that the life-time of the atom is much larger than one orbital period of the electron in the given external field. This latter point is quite important; indeed in strong fields the orbital period can increase with the field strength (for example, for the motion near $\bar{\rho}$, $T = 2\pi/\Omega = 2\pi\epsilon m/\omega^2$) and this may lead to a decrease of the ionization rate which is merely due to a change in the time scale of the problem. We will not consider this as stabilization since after one orbital period the atom will ionize. Therefore our analysis deals with a different regime than in the experiments [13] where the interaction time is of the order of one orbital period. Another important point concerns how the atoms, prepared in a given, initial (Rydberg) state, are injected in the external field or, in other words, how the external field is switched on. As we already discussed we considered situations in which the momentum transfer from the field to the electron during the switching is small ($\int \epsilon(t) dt \approx 0$). Also the switching time is not larger than few orbital periods (otherwise the atom may ionize during the switching process). Therefore under the term stabilization we understand the phenomenon according to which a *given* atomic state with fixed n_0 is stable in a strong field during many orbital periods while it rapidly ionizes in smaller fields.

In [15, 16], the classical dynamics of system (1) has been studied in terms of an approximate map over one period of the external field. The stability of the classical motion is then related to the stability of the fixed points of the map. However, in strong fields, the period of the

driving field is much shorter than the orbital period of the electron $T_{\text{orb}}/T_{\text{ext}} \approx \epsilon m/\omega \gg 1$ and it is questionable whether an analysis over a period shorter than the orbital period is meaningful. Also near the stabilization border, when the two periods are comparable, the approximation by kicks (which include the constant centrifugal force) is not justified. In addition it is not clear whether the map description gives a good approximation for $\alpha_0 = \epsilon_0/\omega_0^2 \ll 1$ since it does not reproduce, for example, the usual chaos border for small fields. In any event, for a correct comparison of different approaches, it is necessary to remark that in Fig. 1 in [15], the two axis ϵ_0 and ω_0 cannot be associated with their usual meaning $\epsilon_0 = \epsilon n_0^4$, $\omega_0 = \omega n_0^3$ with n_0 the initial state. The only way in which Fig. 1 can be correctly understood is to consider $\omega_0 = \omega$ and $\epsilon_0 = \epsilon$, so that $n_0 = 1$ only fixes the classical scale and it is not connected to the initially excited state. This is the reason why destabilization border (7) does not appear in Fig. 1 of [15].

A different approximation to the classical dynamics has been developed [4, 6, 7] on the basis of the 1D model

$$H = \frac{p^2}{2} - \frac{1}{\sqrt{a^2 + z^2}} + \epsilon z \cos \omega t. \quad (10)$$

This model however takes into account only the motion in z direction and neglects the dynamics in ρ which, as discussed above, is the most relevant one in the real 3D atom. In this sense the 1D model (9) gives a more correct description of stabilization and correctly reproduces the stabilization border (5) of the 3D case [11]. Finally, a numerical analysis of the classical problem was carried on also in [17] and led the authors to the conclusion that stabilization takes place in 1D case and not in the 3D case. This result appears to be in contradiction with previous works [1, 9–11, 15, 16].

Our approach to the stabilization problem, discussed in the present paper, is based on classical mechanics and allows us to understand the origin and the conditions of stabilization in strong field. One can now address the question to what extent the above results can be applied to the quantum case. Formally the considerations presented in this paper can be extended to the quantum case if $\omega \ll 1/n_0^2$. However it was shown in [11] that the motion can be described by a simple map, the Kramers map, which is analogous to the Kepler map. The latter describes quite well quantum dynamics even if $\omega > 1/n_0^2$ (for example it gives the correct one-photon ionization rate) [1]. The reason is that the classical map gives also the quasi-classical value of the one photon matrix element which determines the one photon ionization rate via the Fermi golden rule. In the same way the Kramers map determines the quasi-classical value of the matrix element for an one photon transition and gives the one photon ionization rate. According to Kramers map this rate decreases exponentially with the increase of the stabilization parameter S [11], and therefore stabilization persists even in the quantum regime. In conclusion, our classical treatment allows to estimate the quantum ionization rate in the stabilized regime and in particular shows that stabilization takes place even if $\omega \gg 1/n_0^2$.

Different approaches to quantum stabilization have been developed in recent years. In [19] it is argued that

for $\omega > 1/(2n^2)$ the ionization probability of a Rydberg electron will decrease with increase of the field strength provided $\varepsilon > \omega^{5/3}$ (in other words $k > 1$). From our viewpoint this prediction is in contradiction with the Kepler map description which has been confirmed by numerical computations and which is in agreement with quasi-classical limit.

Another condition for stabilization was proposed in [12] and gives $\varepsilon^2/\omega^2 > \omega$. Later, in [14], this condition was modified into $\varepsilon^2/\omega^2 > m\omega$. It is argued that this border is of pure kinematic origin. From our viewpoint, instead, the structure of the average potential is important, since it determines the minimal distance between the electron and the nucleus which actually rules the ionization process. This structure will definitely influence the ionization of Rydberg states at least in the regime when $\omega \ll 1$, $\varepsilon \ll 1$.

In [14] numerical computations are also presented. These computations however do not allow to extract the functional dependence of stabilization border, since the considered parameter range is quite narrow. In this paper the ionization rate is computed from the ground state in the average potential while we consider ionization starting from an excited state in this average potential. Our choice is motivated by the fact that during the switching process the electrons are mainly captured in the excited states of the average potential while the probability to be captured in the ground state is quite small.

One of the important conclusions of our investigations is that stabilization can be obtained not only when the size of the electron oscillations $\alpha = \varepsilon/\omega^2$ is larger than the size of the atom $2n_0^2$, but also in the other limiting case when $\alpha \ll n_0^2$. Our conclusion differs from other results [8] in which stabilization is predicted to occur only when α is larger than the size of the atom. Also in [8] the condition that the photon energy ($\hbar\omega_0$) is larger than ionization energy (E_I) was considered as a necessary condition for stabilization. This condition is of a purely quantum nature and it cannot be satisfied in the quasi-classical limit. According to our results stabilization takes place even for $\hbar\omega_0$ much less than the coupling energy.

A point we would like to stress is that the Rydberg stabilization presented here is a very interesting phenomenon, which we consider more important than the stabilization of atoms in very strong fields, with field strength and frequency larger than the corresponding atomic values ($\varepsilon, \omega \gg 1$). The reason is that in such large fields the ground state is strongly modified and therefore the frequency of transitions between states of a stabilized atom cannot be larger than the atomic unit of energy. Instead in the case of Rydberg stabilization, the field, which is strong enough to stabilize the Rydberg state, does not modify the ground state, since $\varepsilon \ll 1$, $\omega \ll 1$, and it acts as a small perturbation. Therefore the electron energy in the ground state remains approximately the same as for the unperturbed atom while in the Rydberg stabilized state the electron energy can be very high due to fast oscillations in the driving field. Indeed the difference in energy between these two states is of the order of ε^2/ω^2 . For example, for a CO₂ laser with $\omega \approx 1/300$

(0.1 eV) stabilization of Rydberg state with $n_0 = 40$, $m = 2$ takes place for $\varepsilon \sim 2 \cdot 10^8$ V/cm and the transition frequency between the stabilized Rydberg state and the ground state is ~ 1000 eV. It would be very important to estimate the transition rate for the above radiative process. However we think that this rate will be comparable with the transition rate in the normal Rydberg atom, since the size of the atom is the same as for the unperturbed Rydberg state $\alpha = \varepsilon/\omega^2 \lesssim 2n_0^2$. Let us mention that the dipole approximation used above is still correct since the ratio of the wavelength $\lambda = 2\pi c/\omega$ to the size of the atom $2n_0^2$ is approximately 10^2 .

The possibility of radiation of photons with very high energy makes Rydberg stabilization a very interesting phenomenon.

This work has been completed during the E.S.F. workshop "Classical mechanical methods in Quantum mechanics" in Como.

References

1. Casati, G., Guarneri, I., Shepelyansky, D.L.: IEEE J. Quantum Electron. **QE-24**, 1420 (1988)
2. Benvenuto, F., Casati, G., Shepelyansky, D.L.: Phys. Rev. **A45**, 7670 (1992)
3. Gersten, J.I., Mittleman, M.H.: J. Phys. **B9**, 2561 (1976); Mittleman, M.H.: In: Theory of Laser-Atom Interactions. New York: Plenum Press 1982; Gavrilu, M., Kaminski, J.: Phys. Rev. Lett. **52**, 613 (1984); Gavrilu, M.: In: Fundamentals of Laser interactions, Ehloltzky, F. (ed.). Berlin, Heidelberg, New York: Springer 1985
4. Su, Q., Eberly, J.H., Javanainen, J.: Phys. Rev. Lett. **64**, 862 (1990)
5. Su, Q., Eberly, J.H.: Phys. Rev. **A43**, 2474 (1991); Pont, M., Gavrilu, M.: Phys. Rev. Lett. **65**, 2362 (1990); Kulander, K.C., Schafer, K.J., Krause, J.L.: Phys. Rev. Lett. **66**, 2601 (1991); Burnett, K., Knight, P.L., Piraux, B.R.M., Reed, V.C.: Phys. Rev. Lett. **66**, 301 (1991); Reed, V.C., Knight, P.L., Burnett, K.: Phys. Rev. Lett. **67**, 1415 (1991); Dimou, L., Faisal, F.H.M.: Phys. Rev. **A46**, 4442 (1992); Laser Phys. **3**, 440 (1993)
6. Grobe, R., Law, C.K.: Phys. Rev. **A44**, R4114 (1991)
7. Bowden, C.M., Sung, C.C., Pethel, S.D., Ritchie, A.B.: Phys. Rev. **A46**, 592 (1992)
8. Vos, R.J., Gavrilu, M.: Phys. Rev. Lett. **68**, 170 (1992)
9. Benvenuto, F., Casati, G., Shepelyansky, D.L.: Phys. Rev. **A47**, R786 (1993)
10. Shepelyansky, D.L.: Atomic physics, Vol. 13, p. 425, Walther, H., Hansch, T.W., Neizert, B. (eds.). New York: AIP 1993
11. Shepelyansky, D.L.: Phys. Rev. A (submitted for publication)
12. Pont, M., Shakeshaft, R.: Phys. Rev. **A44**, R4110 (1991)
13. Jones, R.R., Bucksbaum, P.H.: Phys. Rev. Lett. **67**, 3215 (1991); Noordam, L.D., Stapelfeldt, H., Duncan, D.I., Gallagher, T.F.: Phys. Rev. Lett. **68**, 1496 (1992)
14. Potvliege, R.M., Smith, P.H.G.: Phys. Rev. **A48**, 46 (1993)
15. Jensen, R.V., Sundaram, B.: Phys. Rev. **A47**, R778 (1993)
16. Jensen, R.V., Sundaram, B.: Phys. Rev. **A47**, 1415 (1993); Laser Phys. **3**, 291 (1993)
17. Gajda, M., Grochmalicki, J., Lewenstein, M., Rzażewski, K.: Phys. Rev. **A46**, 46 (1992); Grochmalicki, J., Lewenstein, M., Rzażewski, K.: Phys. Rev. Lett. **66**, 1038 (1991)
18. Kramers, H.A.: Collected scientific papers, Amsterdam: North Holland 1956; Henneberger, W.C.: Phys. Rev. Lett. **21**, 838 (1968)
19. Fedorov, M.V., Movsesian, A.M.: J. Opt. Soc. Am. **B6**, 928 (1989)